LFM-PSK-based integrated sensing and communication system in the THz band

Zhidong Lyu[1], Lu Zhang[1], Hongqi Zhang[1], Zuomin Yang[1], Lianyi Li[1], Changming Zhang[2], Xianbin Yu[2*]
[1]*College of Information Science and Electronic Engineering, Zhejiang University, 310027 Hangzhou, China*
[2]*Zhejiang Lab, Hangzhou 311121 China*
*E-mail: xyu@zhejianglab.com

***Abstract*—We demonstrate a photonic terahertz integrated sensing and communication (THz-ISAC) system, combining linear frequency modulation and phase-shift keying (LFM-PSK). 20.9 dB peak-to-sidelobe ratio (PSLR) and 6 Gbit/s data rate are simultaneously achieved at 330 GHz.**

Keywords—Terahertz photonics, integrated sensing and communication, linear-frequency modulation and phase-shift keying.

I. Introduction

The wireless transmission system is considered to be evolving from solely relying on communication services to the integrated sensing and communication (ISAC) system, with an expectation to reduce hardware costs and enhance spectrum efficiency [1]. Recently, the terahertz wave (THz, 0.1-10 THz) has emerged as a promising candidate for short-range wireless communication and sensing due to its ultra-broad available bandwidth, which can support both high-resolution sensing and high-capacity communication for the emerging ISAC service [2].

Compared with the electronics-based scheme, the photonic THz-ISAC system has the advantages of large operation bandwidth, electromagnetic interference immunity, as well as transparency to signal modulation formats [3]. Therefore, the design of dedicated waveforms has a critical impact on the photonic THz-ISAC system performance. The research community initially designs the dual-function waveform based on multiplexing schemes, typically frequency division multiplexing (FDM) [4], and time division multiplexing (TDM) [5]. However, these multiplexing schemes are inherently the simple combination of the waveforms, which incur additional resource overhead.

Alternatively, the integrated waveforms tightly couple both time and frequency resources, which is recognized as promising. The radar-centric scenario is one of the typical ISAC scenarios, which is more concerned about the high peak-to-sidelobe ratio (PSLR) and range estimation accuracy, while a limited data rate is acceptable [6]. Recently, research efforts have been put into radar-centric waveform design, through embedding information operation, or the direct spread spectrum (DSS) [7]-[9]. However, the sensing performance of the aforementioned systems is not yet sufficient for radar-centric cases.

In this paper, we propose a photonic radar-centric THz-ISAC system based on the LFM-PSK waveform. Both autocorrelation and practical sensing experiment are conducted, achieving a PSLR as high as 20.9 dB. We also discuss the performance trade-off between the sensing PSLR and range estimation accuracy to calculate the optimal communication data rate, which reaches up to 6 Gbit/s in our experiment.

II. Operation Principle

Fig. 1 illustrates the principle of an integrated LFM-BPSK waveform in the time-frequency domain. The communication symbols $\varphi(t)$ are mapped to additional phases and embedded into the LFM carrier. Thus, the integrated waveform can be expressed as:

$$s(t) = \exp[j\pi(2f_0 t + kt^2) + j\varphi(t)], \tag{1}$$

where f_0 denotes the initial frequency and k is the chirp rate.

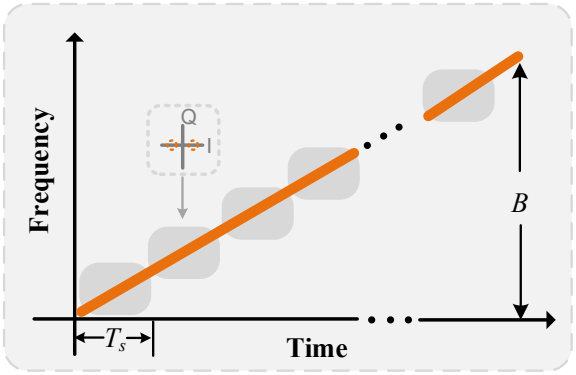

Fig. 1. Schematic for LFM-BPSK waveform generation illustrated in the time-frequency domain.

At the reception side, a matched filter based on pulse compression theory is employed. To eliminate the randomness of the communication symbols, we calculate the expectation of the matched filter output [10]. Assuming the LFM carrier as follows:

$$r_{LFM-BPSK}(\tau) = (T_s - |\tau|)\cdot \mathrm{sinc}[\pi u\tau(T_s - |\tau|)]\cdot \frac{\sin(\pi u\tau T)}{\sin(\pi u\tau T_s)}, \tag{2}$$

where T and T_s represent the time duration of the LFM carrier and a communication symbol, respectively. After being embedded with communication symbols, the LFM-BPSK waveform is close to the noise radar, which has excellent autocorrelation, but its range accuracy is affected by the bandwidth of the transmit signal [11]-[12]. Therefore, we design an optimization problem to maximize the performance gain caused by the BPSK modulation, which can be formulated as:

$$\begin{aligned} &R_{b,opt} = \arg\max_{R_b} \mathrm{PSLR} + \sigma_R \\ &\text{s.t. } R_b < R_{b,th} \end{aligned} \tag{3}$$

where $R_{b,opt}$ and $R_{b,th}$ represent the optimal and the threshold of the data rate, respectively, and σ_R denotes the range estimation error. To unify the dimensions, the PSLR and estimation error should be normalized by the reference signal before being added.

III. Experimental Setup

The experimental setup of the proposed photonic LFM-BPSK THz-ISAC system is depicted in Fig. 2. A continuous lightwave centered at around 1552 nm is emitted from an external cavity laser (ECL), and then launched into a phase modulator (PM) to generate a coherent optical frequency comb (OFC). Here, a polarization controller (PC1) is inserted to optimize the polarization state. The PM is driven by a 33 GHz radio frequency (RF) source, which is amplified by an electrical amplifier with a 38 dB gain. Subsequently, the OFC is fed into a wavelength-selective switch (WSS) to filter out two coherent optical tones with 330 GHz spacing and separately launched into two different branches. Fig. 2(a) shows the optical spectrum of the generated OFC. The optical tone centered at 193.283 THz is first amplified by an Erbium-doped fiber amplifier (EDFA) and then fed into an in-phase and quadrature modulator (IQ-MOD) for the integrated LFM-BPSK waveform modulation, and the other one centered at 192.953 THz serves as the optical local oscillator (LO).

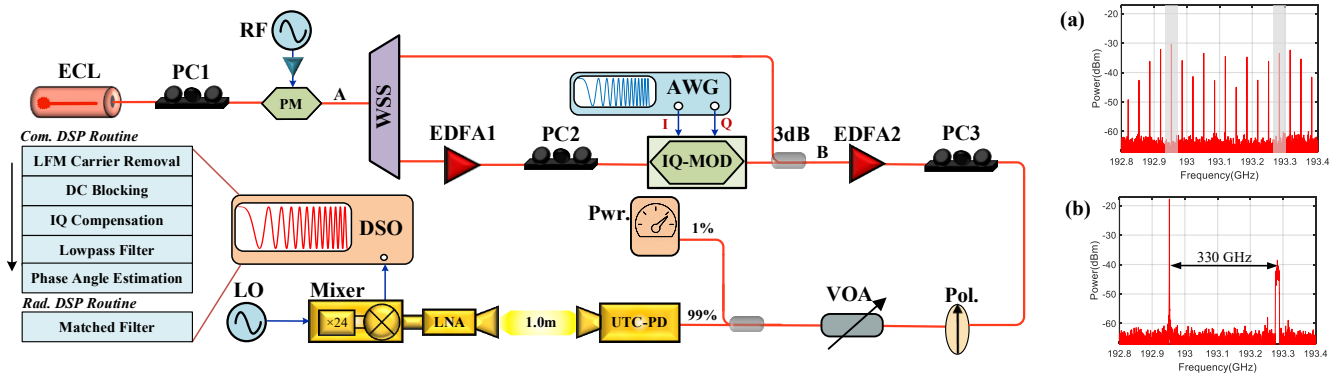

Fig. 2. Experimental setup of the proposed photonic THz-ISAC system based on the LFM-BPSK waveform. ECL: external cavity laser; PC: polarization controller; PM: phase modulator; RF: radio frequency; WSS: wavelength selective switch; EDFA: Erbium-doped fiber amplifier; AWG: arbitrary waveform generator; IQ-MOD: in-phase and quadrature modulator; Pol.: polarizer; VOA: variable optical attenua-tor; Pwr.: power meter; UTC-PD: uni-traveling carrier photodiode; DSO: digital storage oscilloscope; LO: local oscillator. The insert: optical spectrum at (a) point A and (b) point B.

After being embedded with the additional phase, the LFM-BPSK waveform with 12 GHz bandwidth and 2 μs time duration is digital-to-analog converted by an arbitrary waveform generator (AWG, 120 GSa/s) to drive the IQ-MOD. The modulated optical tone is combined with the selected optical LO by a 3 dB optical coupler (OC), as shown in Fig. 2(b). Then, the PC3 and a polarizer are applied to adjust the polarization of the coupled optical signal to maximize the responsivity of a uni-traveling carrier photodiode (UTC-PD). Subsequently, a 330 GHz integrated signal is generated by the UTC-PD with a fixed photocurrent of 3 mA.

The integrated THz signal is transmitted and received by a pair of horn antennas over a 1 m line-of-sight (LOS) wireless link. At the reception side, the received signal is first amplified by a THz low noise amplifier (THz-LNA) with a 22 dB gain. Then, a Schottky mixer is employed for frequency down-conversion, which is driven by a 24-order multiplied electrical LO signal. The output intermediate frequency (IF) signal of the Schottky mixer centered at 21 GHz is analog-to-digital converted by a real-time digital storage oscilloscope (DSO, 160 GSa/s) for further radar and communication processing.

IV. Experimental Results and Discussions

Fig. 3 displays the experimental results. We first analyze the PSLR performance of the proposed LFM-BPSK waveform through the one-dimensional range profile of obtained IF signals. Fig. 3(a) presents the PSLR results in back-to-back, wireless transmission, and theoretical analysis, respectively. As we can see, when the data rate increases from 0 Gbit/s to 6 Gbit/s, the PSLR performance promotes more than 5 dB, with a maximum of 20.9 dB at 6 Gbit/s. The PSLR gain is induced by the randomness of communication symbols, which has the advantage of reducing the masking effect of strong targets [13].

To further validate the superiority of the LFM-BPSK waveform, we also conduct a practical sensing experiment Here, both the transceivers and targets are static. After the digital matched filter process, the obtained range profile is shown in Fig. 3(b). The range profile peak located at 50.0 cm corresponds to the reference mental target, and the other peak at 52.1 cm represents the test target. It is clear that the measured distance between the two targets is 2.1 cm, which is close to the actual value of 2.0 cm. Furthermore, the sidelobe level of the proposed LFM-BPSK waveform is quite lower than the traditional LFM waveform.

Additionally, we further discuss the performance trade-off for the optimal data rate. Fig. 3(c) illustrates the measured PSLR and the mean square error (MSE) of the range estimation, both normalized by the measured corresponding performance of the LFM waveform. We can see that both metrics vary monotonically with the data rate, and the PSLR gain increases more rapidly than the MSE decreases. According to Eq. (3), the optimal data rate for our experiment system should be 6 Gbit/s.

The communication performance of the integrated LFM-BPSK waveform is also evaluated in terms of the bit error rate (BER). After the offline communication processing as shown in the inset of Fig. 2, the communication symbols can be recovered. The transmission BER at different data rates and the eye-diagram at 6 Gbit/s are shown in Fig. 3(d), in the case of back-to-back and wireless transmission. It can be seen, when the data rate varies from 2 Gbit/s to 6 Gbit/s, the BER performance worsens due to the reduction of the signal-to-noise ratio (SNR). Moreover, the measured BER in all cases can reach below the hard-decision forward error correction (HD-FEC) threshold with 7% overhead.

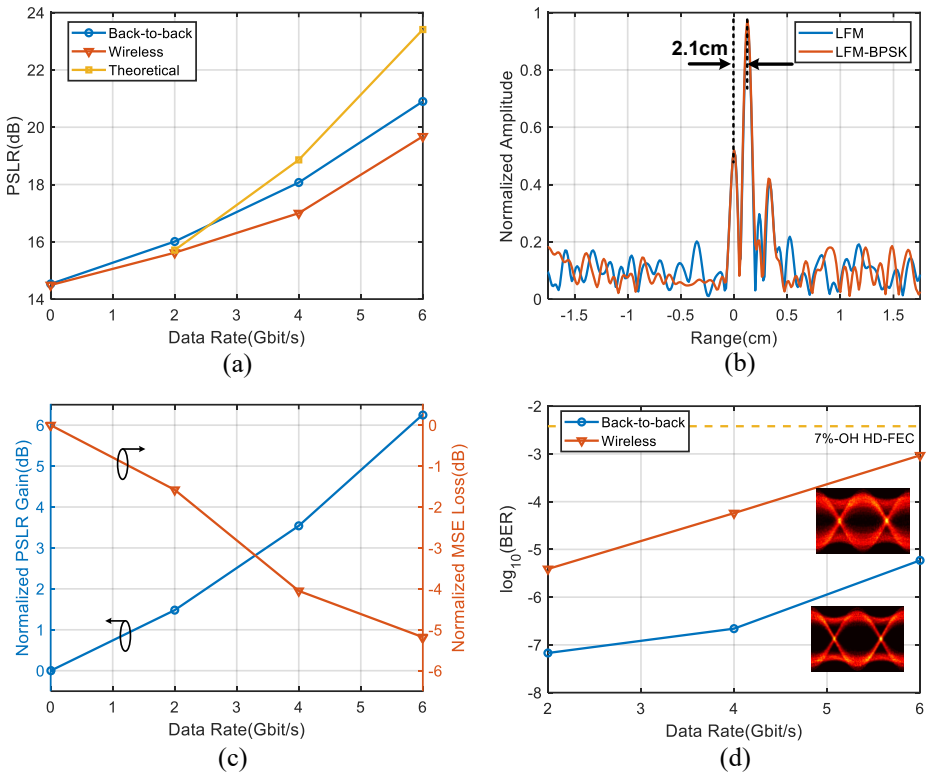

Fig. 3. Experimental results of photonic THz-ISAC system based on the LFM-BPSK waveform. (a) The measured PSLR performance versus data rate. (b) The measured radar range profile for two targets. (c) The normalized PSLR and range estimation MSE versus data rate. (d) The measured BER performance versus the data rate and the eye-diagram.

V. Conclusion

In summary, a photonic THz-ISAC system based on the LFM-BPSK waveform has been proposed and demonstrated, achieving 20.9 dB PSLR and 6 Gbit/s data rate wireless transmission at 330 GHz. We have experimentally confirmed that the randomness of communication symbols can reduce the sidelobe level, with the compromised range estimation accuracy. The performance trade-off of the LFM-BPSK waveform has also been conducted to optimize the communication data rate. The proposed approach provides a promising solution to handle the issue of the masking effect and the optimization for THz-ISAC waveform design.

Acknowledgment

This work is supported by the National Key Research and Development Program of China (2018YFB1801500) and "Pioneer" and "Leading Goose" R&D Program of Zhejiang 2023C01139, in part by the Natural National Science Foundation of China under Grant 62101483, the Natural Science Foundation of Zhejiang Province under Grant LQ21F010015, Zhejiang Lab (no. 2020LC0AD01).

References

[1] A. R. Chiriyath, B. Paul and D. W. Bliss, "Radar-communications convergence: coexistence, cooperation, and co-design," IEEE Trans. Cong. Commun. Netw., vol. 3, no. 1, pp. 1-12, Mar. 2017.

[2] C. Chaccour, M. N. Soorki, W. Saad, M. Bennis, P. Popovski and M. Debbah, "Seven defining features of terahertz (THz) wireless systems: a fellowship of communication and sensing," IEEE Commun. Surv. Tut., vol. 24, no. 2, pp. 967-993, Jan. 2022.

[3] K. Liu et al., "100 Gbit/s THz photonic wireless transmission in the 350-GHz band with extended reach," IEEE Photon. Technol. Lett., vol. 30, no. 11, pp. 1064-1067, Jun. 1, 2018.

[4] S. Jia et al., "A unified system with integrated generation of high-speed communication and high-resolution sensing signals based on THz photonics," J. Lightw. Technol., vol. 36, no. 19, pp. 4549-4556, Oct. 1, 2018.

[5] Y. Wang et al., "Integrated high-resolution radar and long-distance communication based-on photonic in terahertz band," J. Lightw. Technol., vol. 40, pp. 2731-2738, May 1, 2022.

[6] F. Liu et al., "Integrated sensing and communications: Toward dual-functional wireless networks for 6G and beyond," IEEE J. Sel. Areas Commun., vol. 40, no. 6, pp. 1728-1767, Jun. 2022.

[7] H. Nie, F. Zhang, Y. Yang and S. Pan, "Photonics-based integrated communication and radar system," in Proc. MWP, Ottawa, ON, Canada, Oct. 2019, pp. 1-4.

[8] Z. Xue, S. Li, X. Xue, X. Zheng, and B. Zhou, "Photonics-assisted joint radar and communication system based on an optoelectronic oscillator," Opt. Exp., vol. 29, no. 14, pp. 22442-22454, Jul. 2021.

[9] W. Bai et al., "Photonic millimeter-wave joint radar communication system using spectrum-spreading phase-coding," IEEE Trans. Microw. Theory Techn., vol. 70, no. 3, pp. 1552-1561, Mar. 2022.

[10] R. Xie, K. Luo and T. Jiang, "Waveform design for LFM-MPSK-based integrated radar and communication toward IoT applications," IEEE Internet Things J., vol. 9, no. 7, pp. 5128-5141, Apr. 2022.

[11] K. Savci et al., "Noise radar—overview and recent developments," IEEE Aerosp. Electron. Syst. Mag., vol. 35, no. 9, pp. 8-20, Sept. 2020.

[12] U. Pe'er and N. Yang, "Mathematical analysis of the peak sidelobe level of the ambiguity function for random phase codes," IEEE Trans. Aerosp. Electron. Syst., vol. 58, no. 5, pp. 4669-4680, Oct. 2022.

[13] J. S. Kulpa, Ł. Maślikowski and M. Malanowski, "Filter-based design of noise radar waveform with reduced sidelobes," IEEE Trans. Aerosp. Electron. Syst., vol. 53, no. 2, pp. 816-825, Apr. 2017.